1166. Fault diagnosis for rotating machinery based on multi-differential empirical mode decomposition

Han Xiao[1], Jianzhong Zhou[2], Jian Xiao[3], Wenlong Fu[4], Xin Xia[5], Weibo Zhang[6]
College of Hydropower and Information Engineering, Huazhong University of Science and Technology
Wuhan, Hubei, 430074, P. R. China
[2]Corresponding author
E-mail: [2]*jz.zhou@hust.edu.cn*

Abstract. The fault diagnosis of rotating machinery has crucial significance for the safety of modern industry, and the fault feature extraction is the key link of the diagnosis process. As an effective time-frequency method, Empirical Mode Decomposition (EMD) has been widely used in signal processing and feature extraction. However, the mode mixing phenomenon may lead to confusion in the identification of multi frequency signals and restricts the applications of EMD. In this paper, a novel method based on Multi-Differential Empirical Mode Decomposition (MDEMD) was proposed to extract the energy distribution characteristics of fault signals. Firstly, multi-order differential signals were deduced and decomposed by EMD. Then, their energy distribution characteristics were extracted and utilized to construct the feature matrix. Finally, taking the feature matrix as input, the classifiers were applied to diagnosis the existence and severity of rotating machinery faults. Simulative and practical experiments were implemented respectively, and the results demonstrated that the proposed method, i.e. MDEMD, is able to eliminate the mode mixing effectively, and the feature matrix extracted by MDEMD has high separability and universality, furthermore, the fault diagnosis based on MDEMD can be accomplished more effectively and efficiently with satisfactory accuracy.

Keywords: empirical mode decomposition (EMD), energy distribution, multi-differential empirical mode decomposition (MDEMD), fault diagnosis, rotating machinery.

1. Introduction

Large rotating machinery is the essential part of many industrial applications, and the requirement of its safe and uninterrupted operation has become more significant. It is obvious that there is an increasing demand for reliable failure detection and fault diagnosis [1]. Several condition monitoring techniques such as vibration, acoustic and temperature measurements have been investigated for fault feature extraction, and among these techniques vibration measurement and analysis are paid more attention [2-5]. When faults of rotating machinery occur, the vibration signals will present an amplitude modulation phenomenon combining the characteristic frequencies of different defects highly correlative with the structure dynamics, thus, the vibration analysis and feature extraction have great importance for rotating machinery fault diagnosis.

In previous studies, many signal processing methods had been developed to mining the fault characteristic information, such as time-domain analysis, frequency-domain analysis, wavelet transform and empirical mode decomposition. Classical time or frequency domain methods, including the time-domain averaging [6], time-series analysis [7] and frequency spectral analysis [8], were proved to be effective for stationary vibration signals. However, as the vibration signal usually presents non-stationary characteristics in time-domain and diverts energy to a wide spectrum in frequency-domain, these traditional methods cannot sufficiently extract the diagnostic information. Wavelet transform (WT) is a powerful time-frequency method for non-stationary signal analysis by describing the signals on multiple scales with different time-frequency resolution, and it has been widely employed to investigate many kinds of signals [9-12]. The wavelet bases and the decomposition scales are determined in WT, and the frequency components of the decomposition results are only related to the sample frequency, which makes the precision of WT highly influenced by the wavelet selection and restricts its application [13].

Empirical mode decomposition (EMD) is another time-frequency signal processing technique, but different from WT, EMD is a self-adaptive method, which can decompose a non-stationary signal into a series of intrinsic mode functions (IMFs) based on the local characteristics of the signal [14]. In recent years, EMD has been becoming a research focus in signal processing and fault diagnosis [15-25]. Many researchers applied EMD and Hilbert spectrum in the mechanical faults diagnosis and achieved good results [15-18]. A combination of EMD with other signal processing techniques, such as envelope analysis, kernel independent component analysis (KICA), instantaneous dimensionless frequency (DLF) normalization and autoregressive (AR) model, also showed merit in vibration signal processing and feature extraction [19-22]. Meanwhile, according to the specific problems in different application areas, plenty kinds of promotions and modifications including boundary extension, ensemble empirical mode decomposition (EEMD), Multivariate EMD, etc, are proposed to improve the performance of EMD and extended its applications [23-25] vastly.

But unfortunately, the mode mixing phenomena of EMD caused by the signal intermittency and noise disturbance is still one major drawback [26], which may lead to confusion in the extracted features of different faults. To eliminate this defect, in this paper we proposed a feature extraction process based on multi-differential empirical mode decomposition (MDEMD), which employed the EMD to not only the original signal, but also its multi-differential signals, and extracted the energy distribution as the signal characteristics and fault features from the obtained IMFs. As the energy distribution of different frequency components would vary under differential operations, the MDEMD could obtain the fault features with high separability and eliminate the mode mixing phenomena indirectly. To verify the superiority of the proposed method MDEMD, simulative and practical experiments were implemented respectively, and taking the extracted features as input vectors several common classifiers were utilized to process the fault diagnosis.

The rest of the paper is organized as follows: In Section 2, the proposed method multi-differential empirical mode decomposition (MDEMD) is detailed described after the introduction of EMD and energy distribution extraction. In Section 3, simulation experiments are carried out and the effectiveness of MDEMD is verified. In Section 4, MDEMD is applied into the fault diagnosis for rotating machinery, and the results and discussion are given. Section 5 summarizes the conclusions of this work.

2. Multi-differential empirical mode decomposition

2.1. Empirical mode decomposition

EMD is a newly self-adaptive time-frequency technique for non-linear and non-stationary signal processing, which is able to decompose a complex multicomponent signal into a set of intrinsic mode functions (IMFs) satisfying the following two requirements: (1) In the whole set data, the number of extremum and the number of zero-crossings must either be equal or different at most by one; (2) At any point, the mean of the envelope defined by local maxima and the envelope defined by the local minima are zero [14]. Suppose a signal as $x(t)$, and its decomposition procedure is described as follows.

Step 1: Set the original signal $r(t) = x(t)$, and initialize the iteration tag $i = 1$;

Step 2: Find all the local maxima and minima of $r(t)$.

Step 3: Construct the upper envelope $u(t)$ and lower envelope $l(t)$ respectively from the extracted local maxima and minima via the cubic spline curve fitting.

Step 4: Compute the local mean $m(t) = [u(t) + l(t)]/2$, and subtract $m(t)$ from the original signal $r(t)$ to obtain the first component $h(t) = r(t) - m(t)$.

Step 5: Set the new $r(t) = h(t)$, repeat Step 2 to 4 until $h(t)$ meets the requirement of IMF, then design $c_i(t) = h(t)$ as the ith IMF.

Step 6: Subtract $c_i(t)$ from $r(t)$ to obtain the new $r(t) = r(t) - c_i(t)$, if the new $r(t)$

satisfies the stopping criteria, design $r(t)$ as the residue of the signal and stop decomposition process; otherwise, set $i = i + 1$, and repeat from Step 2.

After the decomposition procedure, the investigated signal can be expressed as follows:

$$x(t) = \sum_{i=1}^{n} c_i(t) + r(t),$$ (1)

where n is the amount of IMFs, $c_i(t)$ is the ith IMF, and $r(t)$ is the residue.

2.2. Energy distribution extraction

As mentioned before, the non-stationary vibration signal usually contains a wide spectrum of frequency components, which could be decomposed into a sequence of IMFs with different frequency scales self-adaptably by EMD. Theoretically, the decomposition result is only related to the inherent characteristics of the signal itself, and each IMF contains a different band of frequency components. Through the analysis of IMFs, the implied characteristic information can be revealed, and in this paper, energy distribution is extracted as the signal features.

The energy distribution obtained by estimating the total energy of the signal and energy percentage of each IMF is able to present the frequency construction of the signal. To extract the energy distribution, firstly, the energy of each IMF is computed:

$$E_i = \int_{-\infty}^{+\infty} |c_i(t)^2| dt, \quad i = 1,2, \dots, n.$$ (2)

Then, the energy percentage can be evaluated:

$$EP_i = \frac{E_i}{sum(E_i)}, \quad i = 1,2, \dots, n.$$ (3)

Finally, the total energy of all the IMFs defined as $ET = sum(Ei)$ is combined with the energy percentage to construct the feature vector **FV** $= [ET, EP_1, EP_2, \dots, EP_n]$. It can be noticed that the extracted feature vector **FV** is able to represent the characteristics of a signal in both macroscopic (total energy ET) and microscopic (energy percentage EP_i) ways. Usually, when different signals are investigated, the amount of obtained IMFs can hardly be the same, and a certain number of the chosen IMFs should be decided. In previous studies, it is found out that the most energy of the signal are contained in the first few IMFs, therefore, for single signal analysis, the number m is chosen if the sum energy percentage of the first m IMFs is larger than 95 %, and for multi signals analysis, the largest m is utilized for all the signals, and the feature vector can be expressed as **FV** $= [ET, EP_1, EP_2, \dots, EP_m]$. Particularly, when the amount of IMFs is smaller than m, 0 is assigned to the rest of the vectors.

2.3. Multi-differential EMD and feature extraction

The feature extraction process based on EMD and energy distribution is applicable to signal identification and fault diagnosis, however, its effectiveness is restricted by the mode mixing of EMD. To illustrate this pheromone, a simple example is shown below.

Define two different signals x_1 and x_2 as follows:

$$\begin{cases} x_1(t) = \sin(2\pi t) + 0.05 \cdot \sin(20\pi t), \\ x_2(t) = \sin(2\pi t) + 0.2 \cdot \sin(4\pi t) + 0.05 \cdot \sin(20\pi t). \end{cases}$$ (4)

Obviously, x_2 has more frequency components than x_1, and they are easy to distinguish. Utilize EMD and energy distribution extraction to analyze these two signals, and the IMFs and feature vector **F** are respectively listed in Fig. 1 and Table 1. It can be noticed that x_1 is decomposed into two IMFs: the first one is the higher frequency component, and the other one is the main component, which means the two different frequency components implied in x_1 can be separated from each other quite well by EMD. On the other hand, x_2 is also decomposed into two IMFs, but the first two components of x_2 are both contained in IMF2, which suggests the signal x_2 cannot be decomposed sufficiently by EMD. The undesirable consequence of the mode mixing pheromone is revealed in Table 1, from which it can be seen that the extracted feature vectors of x_1 and x_2 based on EMD are nearly the same, and obviously, the two different signals cannot be identified by these feature vectors.

Table 1. The extracted feature vectors of the signal x_1 and x_2

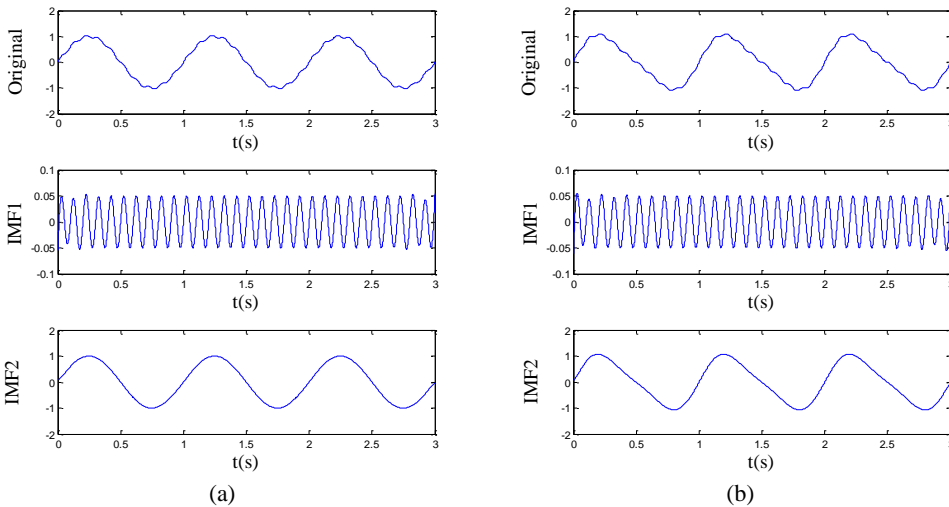| Signal	Features		
	ET	EP_1	EP_2
x_1	$1.50×10^3$	0.0025	0.9975
x_2	$1.56×10^3$	0.0024	0.9976

(a)   (b)

Fig. 1. The EMD result of the signal (a) x_1 and (b) x_2

The most fundamental reason causing the mode mixing is the local extremum selection. One major procedure during the EMD process is calculating the upper and lower envelopes based on the local extremum, and it can be noticed that the amount and the location of the local extremum decides the main frequency components of the current IMF directly. Whether two components can be separated depends on the information of the local extremum. When the frequencies of two components are close, or the amplitude of the higher frequency component is low, the higher frequency component may not generate the local extremum reflecting the real frequency distribution and is hardly to decompose. As is shown in Fig. 1(b), IMF2 contains two components c_1 and c_2 with close frequencies 1 and 2 Hz, and the amplitude of c_2 is much lower, thus c_1 only influences the location of the local extremum, but cannot generate new local extremum, and they haven't been separated.

To eliminate the mode mixing, differential algorithm is introduced into EMD. Theoretically, the differential signal has such properties: (1) it won't change the frequencies of all the components; (2) it will increase the amplitude of component according to its frequency. It is noteworthy that the amplitude increase is linearly related to the frequency of the component, and

according to the previous discussions, such properties are very helpful for improving the EMD. The higher frequency component with low amplitude will be strengthened in the differential signal, and may be able to generate new local extremum. The example above is utilized again to demonstrate the effectiveness of the differential EMD. First, the differential signals of x_1 and x_2 are calculated by central difference as follows:

$$x' = \frac{dx}{dt} = \frac{x(t + \Delta t) - x(t - \Delta t)}{2\Delta t},$$ (5)

where Δt presents a small increments of t, and then, the feature extraction process is carried out with the differential signals.

The result is shown in Fig. 2 and Table 2. Although an undesirable fake IMF appears in Fig. 2(b), the actual components implied in the differential signal of x_2 are decomposed into three IMFs effectively, and extracted feature vectors listed in Table 2 can be noticed to have high separability. Additionally, when the EMD result of the 1st-order differential signal still cannot separate the different frequency components, the 2nd-order and higher-order differential signals could be utilized:

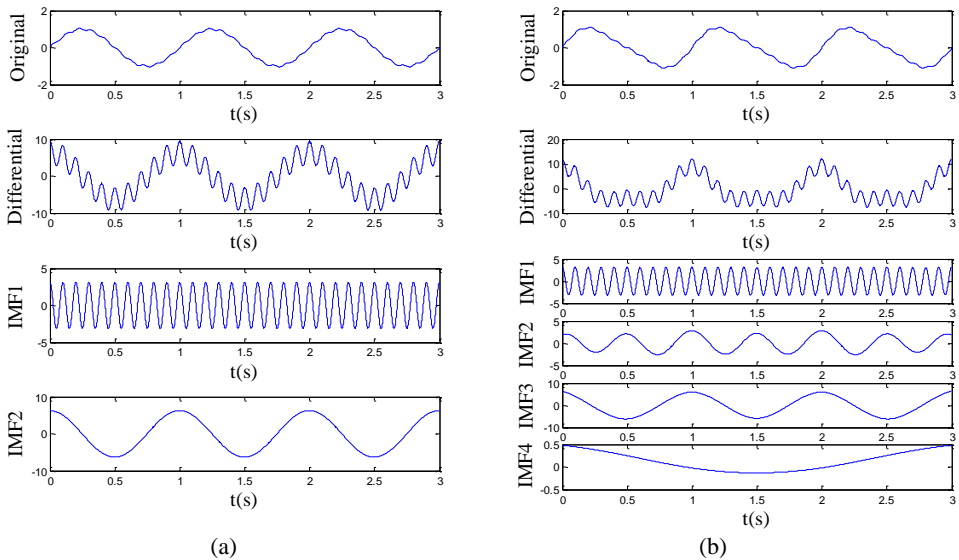$$x^{(n)} = \frac{d^n x}{dt^n} = \frac{x^{(n-1)}(t + \Delta t) - x^{(n-1)}(t - \Delta t)}{2\Delta t}.$$ (6)

(a)   (b)

Fig. 2. The differential EMD result of the signal (a) x_1 and (b) x_2

Table 2. The extracted feature vectors of the signal x_1 and x_2 by differential EMD

Signal	Features				
	ET	EP_1	EP_2	EP_3	EP_4
x_1	6.10×10^4	0.2000	0.8000	0.0000	0.0000
x_2	5.53×10^4	0.1939	0.1150	0.6688	0.0023

Based on the above studies, a novel Multi-Differential EMD (MDEMD) method is proposed to improve the effectiveness of the signal decomposition and feature extraction by combining the energy distribution characteristics of multi-order differential signals, and the flow chart of MDEMD is shown in Fig. 3. Multi-order differential signals are obtained, and the energy distribution features of these signals are extracted respectively. To represent the signal more

comprehensively, all the extracted feature vectors are combined to construct the feature matrix. During the MDEMD process, the higher order is chosen, the more frequency information could be obtained, but the high order differential operation may lead to serious signal distortion. Therefore, the max order of multi-order differential signal N should be decided by the complexity of the investigated signal.
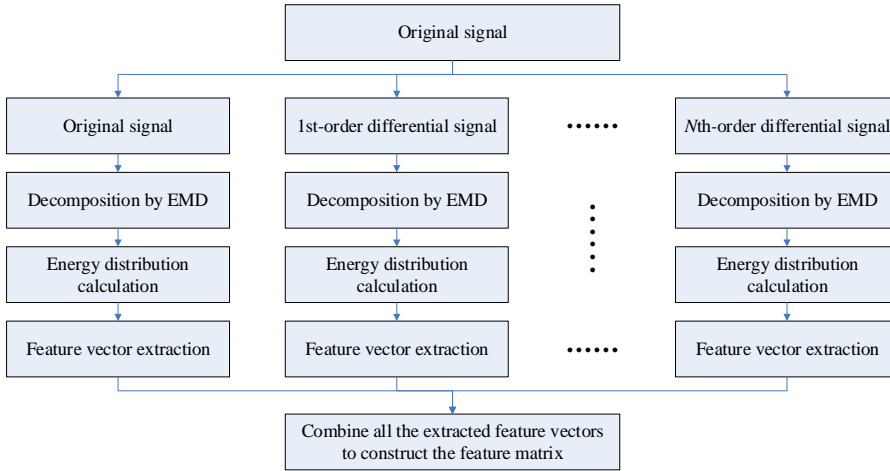

Fig. 3. The flow chart of MDEMD

3. Simulation experiment

3.1. Simulation signals

In this section, artificial signals are constructed to simulate the vibration signals of rotating machinery, and the simulation experiment is implemented to verify the superiority of the proposed MDEMD method. A set of signal components are defined in Eq. 4, and a certain combination of them can simulate the vibration response of the corresponding fault [18].

$$\begin{cases} e_1(t) = \sin(2\pi \cdot 60t), \\ e_2(t) = \big(1 + 0.1\sin(2\pi \cdot 15t)\big)\sin\big(2\pi \cdot 120t + 0.2\sin(2\pi \cdot 10t)\big), \\ e_3(t) = \sin(2\pi \cdot 240t), \\ e_4(t) = \sin(2\pi \cdot 360t), \\ e_5(t) = \text{noise}, \end{cases} \tag{7}$$

where $e_1(t)$ is a sinusoidal signal with the frequency of 60 Hz representing the $1X$ component, $e_2(t)$ is an intra-wave modulated signal representing the $2X$ harmonic component, $e_3(t)$ and $e_4(t)$ are both sinusoidal signals representing the $4X$ and $6X$ harmonic components, and $e_5(t)$ is the noise signal. Previous researches have found that the $1X$ vibration is often caused by mass unbalance, and the excitation source of $2X$ vibration harmonic is usually misalignment, while the $4X$ and $6X$ vibration harmonic components constantly appear in the response of rubbing fault. In the simulation experiment, four classes of signals with different combinations of $e_1(t) - e_5(t)$ are established as follows:

$$\begin{cases} x_1(t) = e_1(t) + e_5(t), \\ x_2(t) = e_1(t) + A \cdot e_2(t) + C \cdot e_4(t) + e_5(t), \\ x_3(t) = e_1(t) + B \cdot e_3(t) + C \cdot e_4(t) + e_5(t), \\ x_4(t) = e_1(t) + A \cdot e_2(t) + B \cdot e_3(t) + C \cdot e_4(t) + e_5(t), \end{cases} \tag{8}$$

where A is a random number in the range of [0.3, 0.4], B is a random number in the range of [0.28, 0.32], and C is a random number in the range of [0.09, 0.11]. Forty samples for each class are produced with different A, B, C, 25 of which are training samples and the other are testing samples. Fig. 4 gives a set of examples of the four classes.
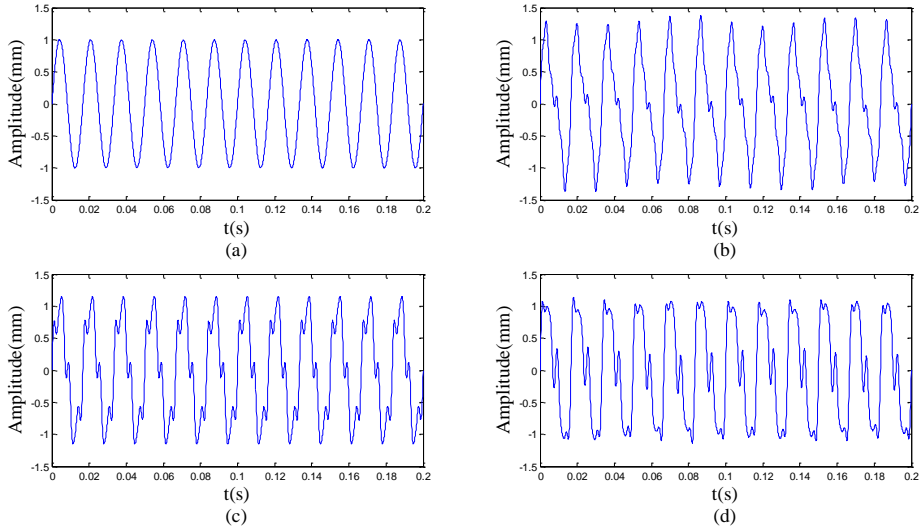

Fig. 4. Examples of the four classes: (a) x_1, (b) x_2, (c) x_3 and (d) x_4

3.2. Signal decomposing and feature extraction analysis

In the simulation experiment, the max-order of MDEMD is set to 2, and EMD is applied to the original and multi-order differential signals. As the amplitude of signal would change after the differential operation, in order to make the extracted energy distribution more convincing, the differential signal is divided by a determined factor equals to 120π, so that the amplitude of $1X$ component would keep invariant. The main IMFs obtained by EMD of the example signals are respectively shown in Fig. 5 to 7.
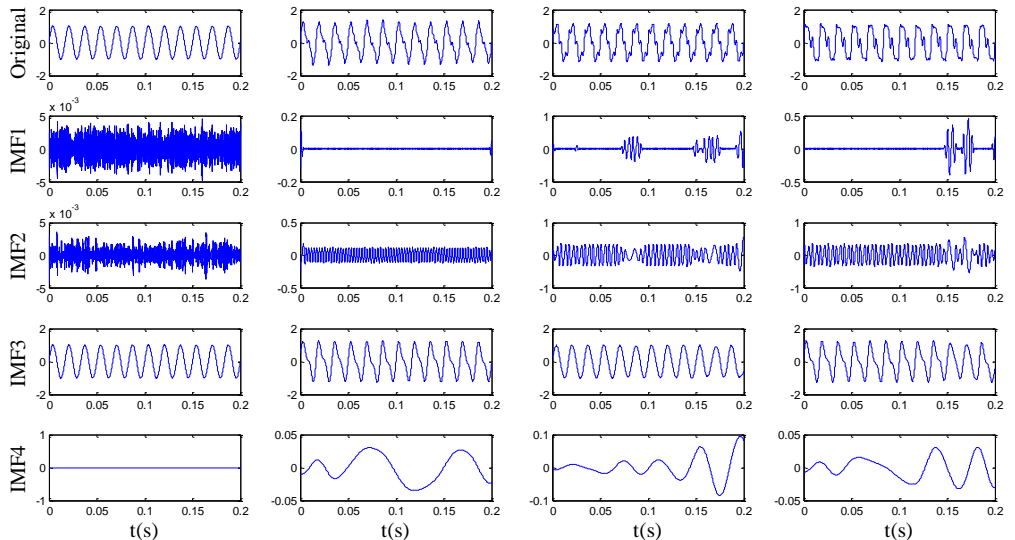

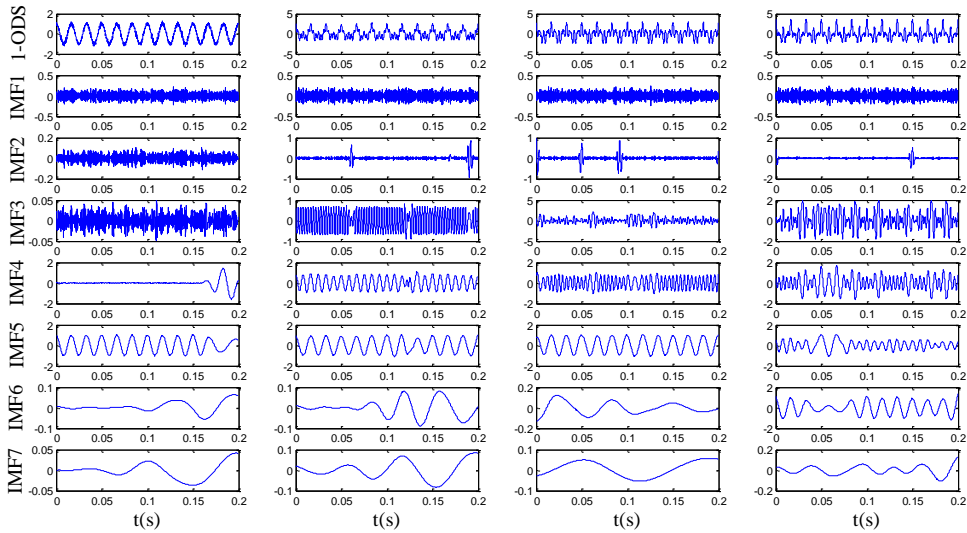**Fig. 5.** The decomposition result of the original signals

Fig. 6. The decomposition result of the 1-order differential signals (1-ODS)
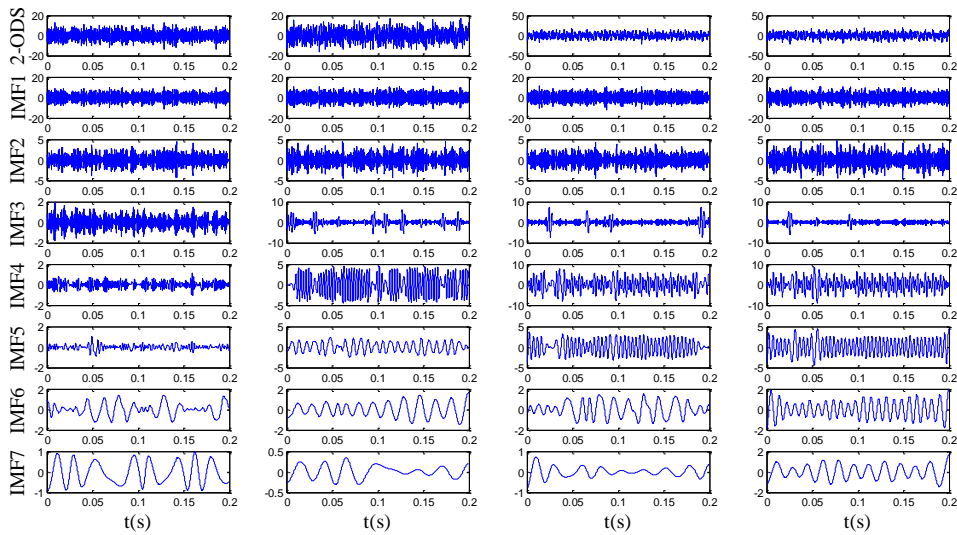

Fig. 7. The decomposition result of the 2-order differential signals (2-ODS)

In Fig. 5 it is revealed that multiple frequency components contained in the simulation samples cannot be decomposed sufficiently by EMD and the mode mixing exists evidently. For example, the IMF3 of signal $x_2(t)$ and $x_4(t)$ contains $1X$ and $2X$ components, and the IMF2 of $x_1(t)$ contains $4X$ and $6X$ harmonic components. In Fig. 6 and 7, the amplitude of higher frequency components rises more obviously through the differential process, and the influence of noise signals becomes more serious. However, although the smoothness of the signals decreases, the multiple frequency components implied in the multi-order differential signals can be decomposed more sufficiently.

Based on decomposition results, the feature matrixes of energy distribution are extracted and parts of them are listed in Table 3. Through comparison of the feature vectors extracted from multi-order differential signals, it is revealed that the energy distributions of four original signals are quite similar to each other, while the energy distributions of 1- and 2-order differential signals have quite big differences.

Table 3. The extracted feature matrixes of the four examples

Signal		Features matrix								
		ET	EP_1	EP_2	EP_3	EP_4	EP_5	EP_6	EP_7	EP_8
x_1	Original	1.00×10^3	0.000	0.000	1.000	0.000	0.000	0.000	0.000	0.000
	1-ODS	9.47×10^2	0.010	0.002	0.001	0.222	0.761	0.001	0.001	0.000
	2-ODS	2.81×10^4	0.838	0.093	0.018	0.006	0.003	0.023	0.017	0.001
x_2	Original	1.17×10^3	0.000	0.010	0.987	0.001	0.001	0.001	0.000	0.000
	1-ODS	1.18×10^3	0.008	0.012	0.206	0.334	0.436	0.002	0.002	0.000
	2-ODS	3.68×10^4	0.598	0.063	0.083	0.189	0.049	0.017	0.001	0.000
x_3	Original	9.84×10^2	0.027	0.080	0.890	0.002	0.000	0.000	0.001	0.000
	1-ODS	1.52×10^3	0.005	0.015	0.372	0.224	0.377	0.003	0.001	0.003
	2-ODS	3.79×10^4	0.486	0.048	0.066	0.292	0.088	0.017	0.002	0.001
x_4	Original	1.17×10^3	0.009	0.080	0.907	0.001	0.002	0.001	0.000	0.000
	1-ODS	1.96×10^3	0.005	0.008	0.393	0.279	0.107	0.204	0.001	0.003
	2-ODS	4.10×10^4	0.506	0.062	0.025	0.273	0.100	0.019	0.013	0.002

To verify the separability of the extracted features, Support Vector Machine (SVM), which is a common pattern recognition method based on the structural risk minimization (SRM) principle [27], is applied to identify the four classes of simulation signals with the energy distribution characteristics respectively obtained by the original EMD, 1- and 2-order MDEMD. The identification results are summarized in Table 4. By the original EMD method, the identification rates of the four classes are quite different and the average identification rates of training and testing samples are respectively 67.7 and 65.3 %, which are too low for the signal identification. By the 1-order MDEMD, all the identification rates are significantly improved, and the average identification rates rise to 93.9 and 94.2 %. By the 2-order MDEMD, the accuracy is further improved, and the identification rates of three classes have reached 100 %. The simulation experimental result verifies the separebility of the extracted features and demonstrates that the proposed MDEMD method is suitable for signal identification.

Table 4. The identification results

Class of signals	Accuracy of EMD		Accuracy of 1-order MDEMD		Accuracy of 2-order MDEMD	
	Training	Testing	Training	Testing	Training	Testing
x_1	48.0 %	50.6 %	86.4 %	85.3 %	100 %	100 %
x_2	82.4 %	82.0 %	100 %	100 %	100 %	100 %
x_3	80.0 %	72.0 %	89.2 %	91.3 %	92.4 %	92.0 %
x_4	60.4 %	56.7 %	100 %	100 %	100 %	100 %
Average	67.7 %	65.3 %	93.9 %	94.2 %	98.1 %	98.0 %

4. Applications in fault diagnosis for rotating machinery

4.1. Data collection

Rolling element bearings are the major part of most rotating machineries, and detecting and diagnosing the existence and severity of bearing faults is significant to prevent the rotating mechanical system from fatal breakdowns. In this section, the proposed MDEMD method is applied to feature extraction and fault diagnosis for rolling element bearings.

Part of the bearings vibration dataset collected by K. A. Loparo [28] is used in this paper. Three faults including outer race fault, inner race fault and ball fault, with the same defect sizes of 0.007 or 0.021 in, were respectively introduced into the drive-end bearing of the motor, which were tested under four different loads, 0, 1, 2 and 3 hp and the vibration data was collected at 12000 samples/s and 24000 samples/s by the installed sensors. In this paper, the vibration data collected at 12000 samples/s under 0 hp load with the defect sizes of 0.007 or 0.021 in was utilized and divided into 100 sub-signals with 4096 data points for each group. The produced 6 classes of

samples covering 6 types of faults are listed in Table 5, and their time responses are illustrated in Fig. 8.

Table 5. Description of bearing fault dataset

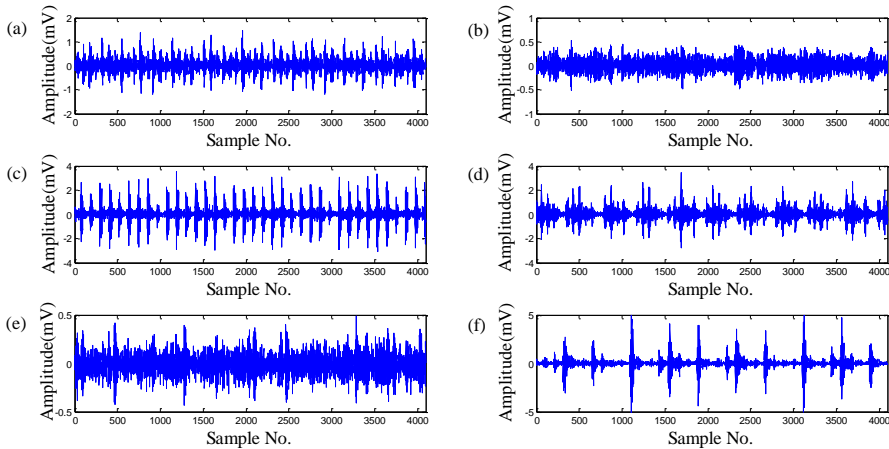| The number of fault samples	Defect size (in)	Position of fault	Label of class
100	0.007	Out race	F_1
100	0.007	Inner race	F_2
100	0.007	Ball	F_3
100	0.021	Out race	F_4
100	0.021	Inner race	F_5
100	0.021	Ball	F_6

Fig. 8. Time series of fault signals: (a) ball fault with 0.007 in; (b) inner race fault with 0.007 in; (c) outer race fault with 0.007 in; (d) ball fault with 0.021 in; (e) inner race fault with 0.021 in; (f) outer race fault with 0.021 in

4.2. Feature extraction and fault diagnosis

Based on the theories above, the energy distribution characteristics of all the samples are extracted from the original and multi-order differential signals respectively, and the length of the extracted feature vectors is set to 10 containing 1 ET and 9 EPs. After feature extraction, the obtained feature matrixes were scaled to be in [0, 1].

The fault diagnosis experiments were carried out with the fault features respectively extracted by the original EMD, 1- and 2-order MDEMD, and half of the samples for each class were randomly selected as training data leaving the rest as testing data. Furthermore, the four most common classifiers including k-Nearest Neighbor algorithm (kNN), Radial Basis Function (RBF) Neural Network, Support Vector Machine (SVM) and Probabilistic Neural Network (PNN) were applied to identify the 6 classes of faults, and the experiment of each method was repeated for 30 times.

Table 6 shows the comparison results of different diagnostic methods, and the identification rates of training and testing samples are reported respectively. It is clear that, the testing accuracy of 1-order MDEMD is much higher than the original EMD and reaches to more than 98.70 %, while the identification rate of 2-order MDEMD is further increased to more than 99 %. It is also noticed that the identification accuracies of different classifiers varied in a small range. The minimum testing accuracy by using original EMD is 92.11 % for RBF while the maximum is 95.68 % for PNN, and the variance is 3.57 %. By using 1-order MDEMD, the minimum and maximum testing accuracies are respectively 98.70 and 99.33 % corresponding to RBF and PNN, and the variance deduced to only 0.63 %. Especially, by utilizing 2-order MDEMD the lowest

accuracy is 99.04 % for kNN, and the identification rates of SVM and PNN are nearly 100 %. Therefore the effectiveness and universality of the proposed MDEMD are demonstrated.

Table 6. The fault identification rates of different methods

Method	Identification rate of training samples (%)			Identification rate of testing samples (%)		
	Original EMD	1-order MDEMD	2-order MDEMD	Original EMD	1-order MDEMD	2-order MDEMD
kNN	95.63	98.76	99.27	94.47	98.72	99.04
RBF	93.54	98.91	99.81	92.11	98.70	99.46
SVM	94.93	99.25	99.95	94.56	99.03	99.80
PNN	98.50	100	100	95.68	99.33	99.86

Meanwhile, it is noteworthy that the higher order for MDEMD would produce lager feature matrix, and the time consumption would increase accompanied with the accuracy, thus, the selection of the proper order depends on the balance between the requirements of the accuracy and efficiency. For the fault diagnosis of rotating machinery, the recommended max order is 2. In summary, the comparison results reflect that MDEMD can stably extract the fault features with high separabilities and the fault diagnosis can be completed with satisfactory accuracy by using these fault features. It is feasible for fault diagnosis of rotating machinery.

5. Conclusion

In this paper, a novel method of feature extraction based on Multi-Differential Empirical Mode Decomposition for fault diagnosis of rotating machinery was proposed and described, where the feature matrix of energy distribution is extracted from the EMD results of multi-order differential signals automatically. Simulation experiment was implemented with four classes of signals containing different frequency components, and the decomposition results and extracted features were described and discussed. Meanwhile, six classes of fault datasets for the rolling element bearings were utilized in the practical experiment, and the fault features are extracted by different order MDEMD and identified by four most common classifiers. The diagnosis results were compared with the original EMD in both training and testing identification rates. The experimental results showed that the proposed method is suitable for the feature extraction of rotating machinery, and it is an important support for realizing automatic fault diagnosis with satisfactory accuracy.

Acknowledgements

References

[1] **Liu T., Chen J., Dong G. M., Xiao W. B., Zhou X. N.** The fault detection and diagnosis in rolling element bearings using frequency band entropy. Proceedings of the Institution of Mechanical Engineers, Part C: Journal of Mechanical Engineering Science, Vol. 227, Issue 1, 2012, p. 87-99.
[2] **Lee H.** Sound radiation from in-plane vibration of thick annular discs with a narrow radial slot. Proceedings of the Institution of Mechanical Engineers, Part C: Journal of Mechanical Engineering Science, Vol. 227, Issue 5, 2012, p. 919-934.
[3] **Dong G. M., Chen J.** Noise resistant time frequency analysis and application in fault diagnosis of rolling element bearings. Mechanical Systems and Signal Processing, Vol. 33, 2012, p. 212-236.
[4] **Castro de H. F., Cavalca K. L., Camargo de L. W. F., Bachschmid N.** Identification of unbalance forces by metaheuristic search algorithms. Mechanical Systems and Signal Processing, Vol. 24, 2010, p. 1785-1798.

[5]   **Xiang X. Q., Zhou J. Z., An X. L., Peng B., Yang J. J.** Fault diagnosis based on Walsh transform and support vector machine. Mechanical Systems and Signal Processing, Vol. 22, 2008, p. 1685-1693.
[6]   **McFadden P. D.** Examination of a technique for the early detection of failure in gears by signal processing of the time domain average of the meshing vibration. Mechanical Systems and Signal Processing, Vol. 1, 1987, p. 173-183.
[7]   **Wang C., Kang Y., Shen P., Chang Y., Chung Y.** Applications of fault diagnosis in rotating machinery by using time series analysis with neural network. Expert Systems with Applications, Vol. 37, 2010, p. 1696-1702.
[8]   **Sanza J., Pererab R., Huertab C.** Fault diagnosis of rotating machinery based on auto-associative neural networks and wavelet transforms. Journal of Sound and Vibration, Vol. 302, 2007, p. 981-999.
[9]   **Newland D. E.** An introduction to random vibrations, Spectral & Wavelet Analysis. Third ed., Longman Scientific & Technical, England, 2005.
[10]   **Zhang Y. P., Huang S. H., Hou J. H., Tao S., Wei L.** Continuous wavelet grey moment approach for vibration analysis of rotating machinery. Mechanical Systems and Signal Processing, Vol. 20, 2006, p. 1202-1220.
[11]   **Abbasion S., Rafsanjani A., Farshidianfar A., Irani N.** Rolling element bearings multi-fault classification based on the wavelet denoising and support vector machine. Mechanical Systems and Signal Processing, Vol. 21, 2007, p. 2933-2945.
[12]   **Al-Badour F., Sunar M., Cheded L.** Vibration analysis of rotating machinery using time-frequency analysis and wavelet techniques. Mechanical Systems and Signal Processing, Vol. 25, 2011, p. 2083-2101.
[13]   **Dou D. Y., Yang J. G., Liu J. T., Zhao Y. K.** A rule-based intelligent method for fault diagnosis of rotating machinery. Knowledge-Based Systems, Vol. 36, 2012, p. 1-8.
[14]   **Huang N. E., Shen Z., Long S. R.** The empirical mode decomposition and the Hilbert spectrum for non-linear and non-stationary time series analysis. Proc. R. Soc. Lond., Vol. 454, 1998, p. 903-995.
[15]   **Liu B., Riemenschneider S., Xu Y.** Gearbox fault diagnosis using empirical mode decomposition and Hilbert spectrum. Mechanical Systems and Signal Processing, Vol. 20, Issue 3, 2006, p. 718-734.
[16]   **Qin Y., Qin S. R., Mao Y. F.** Research on iterated Hilbert transform and its application in mechanical fault diagnosis. Mechanical Systems and Signal Processing, Vol. 22, Issue 8, 2008, p. 1967-1980.
[17]   **Yang Y., He Y. G., Cheng J. S., Yu D. J.** A gear fault diagnosis using Hilbert spectrum based on MODWPT and a comparison with EMD approach. Measurement, Vol. 42, Issue 4, 2009, p. 542-551.
[18]   **Xiong X., Yang S. X., Gan C. B.** A new procedure for extracting fault feature of multi-frequency signal from rotating machinery. Mechanical Systems and Signal Processing, Vol. 32, 2012, p. 306-319.
[19]   **Tsao W. C., Li Y. F., Le D. D., Pan M. C.** An insight concept to select appropriate IMFs for envelope analysis of bearing fault diagnosis. Measurement, Vol. 45, 2012, p. 1489-1498.
[20]   **Li Z. X., Yan X. P., Tian Z., Yuan C. Q., Peng Z. X., Li L.** Blind vibration component separation and nonlinear feature extraction applied to the nonstationary vibration signals for the gearbox multi-fault diagnosis. Measurement, Vol. 46, 2013, p. 259-271.
[21]   **Wu T. Y., Chen J. C., Wang C. C.** Characterization of gear faults in variable rotating speed using Hilbert-Huang Transform and instantaneous dimensionless frequency normalization. Mechanical Systems and Signal Processing, Vol. 30, 2012, p. 103-122.
[22]   **Wang Y. J., Kang S. Q., Jiang Y. C., Yang G. X., Song L. X., Mikulovich V. I.** Classification of fault location and the degree of performance degradation of a rolling bearing based on an improved hyper-sphere-structured multi-class support vector machine. Mechanical Systems and Signal Processing, Vol. 29, 2012, p. 404-414.
[23]   **Parey A., Pachori R. B.** Variable cosine windowing of intrinsic mode functions: Application to gear fault diagnosis. Measurement, Vol. 45, 2012, p. 415-426.
[24]   **Wu Z. H., Huang N. E.** Ensemble empirical mode decomposition: a noise assisted data analysis method. Adv. Adapt. Data Analysis, Vol. 1, 2009, p. 1-41.
[25]   **Zhao X. M., Patel T. H., Zuo M. J.** Multivariate EMD and full spectrum based condition monitoring for rotating machinery. Mechanical Systems and Signal Processing, Vol. 27, 2012, p. 712-728.
[26]   **Bao F., Wang X. L., Tao Z. Y.** EMD-based extraction of modulated cavitation noise. Mechanical Systems and Signal Processing, Vol. 24, 2010, p. 2124-2136.
[27]   **Vapnik V. N.** The Nature of Statistical Learning Theory. Springer-Verlag, New York, 1999.
[28]   **Loparo K. A.** Bearings vibration dataset. Case Western Reserve University, 2011, http://www.eecs.case.edu/laboratory/bearing/download.htm.